Model Predictive Lateral Vehicle Guidance Using a Position Controlled EPS System

Jochen Gallep * **Vivan Govender** ** **Steffen Müller** ***

* *Department of Automotive Engineering, Technical University of Berlin, Berlin, Germany, (e-mail: jochen.gallep@tu-berlin.de)*
** *Daimler AG, Böblingen, Germany, (e-mail: vivan.govender@daimler.com)*
*** *Department of Automotive Engineering, Technical University of Berlin, Berlin, Germany, (e-mail: steffen.mueller@tu-berlin.de)*

Abstract: On the way to automated driving it is necessary to develop suitable control structures which ensure an accurate and robust path tracking during different maneuvers and speeds. This paper presents a Model Predictive Controller (MPC) for lateral vehicle guidance which calculates an optimal manipulated variable sequence for an inner low level steering angle controller of an Electric Power Steering (EPS). On the basis of prior work, a linear controller design is used to control the front steer angle and the resulting steering control loop behaviour is explicitly considered in the prediction model of the outer MPC. The MPC uses a speed-dependent adaptation of the prediction model and the cost function weights to ensure a stable and precise path tracking performance. The MPC real-time capability will be assessed and the performance of the proposed controllers evaluated.

Keywords: Autonomous vehicles, linear time-varying MPC, path tracking, steering angle control, electric power steering, steering analysis

1. INTRODUCTION

The lateral guidance of autonomous vehicles using Electric Power Steering (EPS) systems places high demands on the control accuracy of the lateral controller. This includes, in particular, a good reference tracking during different driving maneuvers to avoid potential dangerous situations. In order to reduce the lateral displacement while taking into consideration the future heading angle as well as EPS limitations, optimal reference steering angles values need to be calculated. The first step of the optimal control sequence is then used as an input for the subordinated steering angle controller. Due to the absence of a human driver, the steering wheel is free moving, which changes the steering system dynamics compared to a non-autonomous vehicle. These new steering dynamics is controlled using an angle controller, that ensures a predictable and accurate steering position control that can be considered in the outer lateral controller.

A possible control strategy for the outer lateral controller in the context of autonomous driving is Model Predictive Control (MPC). MPC honours constraints of the steering angle δ and steering angle velocity $d\delta/dt$ during the calculation of the optimal manipulated variable sequence. Because of the receding horizon principle, future course information is taken into account. Keviczky et al. (2006) introduces a MPC with nonlinear prediction model for lateral vehicle guidance. The calculation of the nonlinear optimization problem causes a high computational burden, which is a drawback for practical implementations. Katriniok and Abel (2011) and Turri et al. (2013) thus use linearizations of the nonlinear prediction model to calculate the manipulated variable. Additionally the calculation of the lateral displacement references to the vehicles center of gravity. Within their work, the controller performance is tested with lane change and evasive maneuvers at a constant speed of 15 m/s.

In experimental test vehicles the position of the center of gravity is load-dependent and therefore not precisely known without prior measurements. Thus a clearly defined geometric reference point on the vehicle is used such as the intersection between the central axis and the front axle axis.

Within this work, the influence of the reference point on the controller design and controller performance will be examined. Furthermore, the operating area of the controller will be extended to different maneuvers and velocities. The focus will be on low speeds ($1 - 2$ m/s) with small curve radius (< 10 m) as they occur during parking and manoeuvring through narrow spaces. An addition focus is on high dynamic manoeuvres at increased speed.

2. SYSTEM OVERVIEW

Figure 1 shows the path control system consisting of Vehicle, EPS and the MPC lateral controller. The reference heading angle $\Theta_{ref} = arctan(dy/dx)$ is calculated on the basis of the reference path information in xy-coordinates, which the car needs to follow.

The MPC receives the actual velocity v, yaw rate $\dot{\psi}$, yaw angle ψ, lateral displacement dy and the steering angle at the front axle δ. The MPC manipulated variable

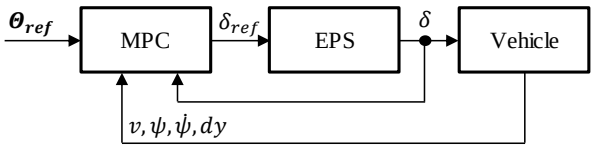

Fig. 1. Path control system

commands δ_{ref} are propagated to a subordinated steering angle controller inside the EPS.

3. PREDICTION MODEL

An important element of the MPC is the prediction model, which is used to predict the future vehicle behaviour. The key objective is to predict the lateral displacement dy for future manipulated variable commands δ_{ref}. Figure 2 shows all relevant variables for the prediction of dy. The variable v_v represents the velocity vector of the front wheel which encloses the angle γ relative to the inertial system.

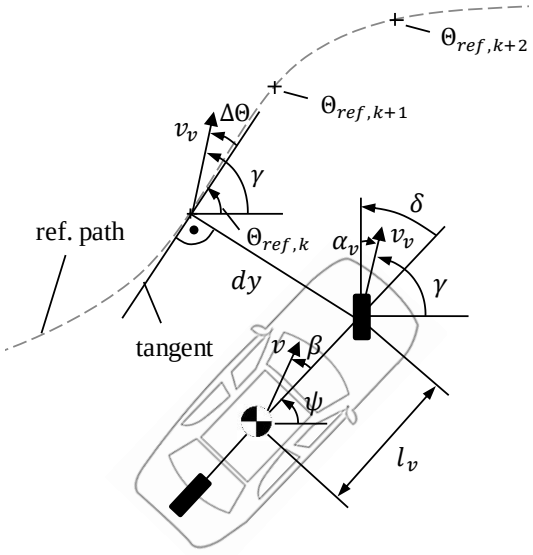

Fig. 2. Single track model and reference path

The discrete reference heading angle sequence $\Theta_{ref,k+i}$ represents the discrete reference heading angles for discrete time steps ahead of the vehicle. On the Basis of trigonometrical relationships the angle γ is calculated according to the following expressions:

$$tan(\delta - \alpha_v) = \frac{vsin\beta + l_v\dot{\psi}}{vcos\beta} \approx \beta + l_v\frac{\dot{\psi}}{v} \tag{1}$$

$$\Rightarrow \gamma = \psi + \delta - \alpha_v = \psi + \beta + l_v\frac{\dot{\psi}}{v}. \tag{2}$$

The lateral displacement rate results from the velocity v_v and small heading angle errors $\Delta\Theta = \gamma - \Theta_{ref}$ to:

$$\begin{aligned} d\dot{y} &= v_v sin(\gamma - \Theta_{ref}) \approx v(\gamma - \Theta_{ref}) \\ &= v(\psi + \beta + l_v\frac{\dot{\psi}}{v} - \Theta_{ref}). \end{aligned} \tag{3}$$

The calculation of the states $\dot{\psi}$ and β will be performed through a dynamic and a kinematic single-track model. The kinematic model describes the vehicle dynamics less accurately, but can be simply parametrized because it uses the wheel base as the only vehicle parameter and the model can also be used in case of zero velocity.

3.1 Kinematic Single Track Model

Ignoring vehicle mass and inertia, $\dot{\psi}$ and β are geometrically defined using Ackermann steering angle and can be written as

$$\dot{\psi} = \frac{v}{R} = v\frac{\delta}{L} \tag{4}$$

$$\beta \approx \frac{L}{2R} = \frac{\delta}{2}. \tag{5}$$

R corresponds to the curve radius and $L = l_v + l_h$ to the wheelbase.

3.2 Dynamic Single Track Model

The linear single-track model according Mitschke and Wallentowitz (2014) describes the lateral vehicle dynamics with a state-space representation and the parameters cornering stiffness (c_α), mass moment of inertia around the vertical axis (J), vehicle mass (m) and the distances between CoG and front/rear axle (l_v, l_h) as follows:

$$\frac{d}{dt}\begin{bmatrix}\dot{\psi}\\ \beta\end{bmatrix} = \begin{bmatrix}a_{1,1}(v) & a_{1,2}\\ a_{2,1}(v) & a_{2,2}(v)\end{bmatrix}\begin{bmatrix}\dot{\psi}\\ \beta\end{bmatrix} + \begin{bmatrix}\frac{c_{\alpha,v}l_v}{J}\\ \frac{c_{\alpha,v}}{vm}\end{bmatrix}\delta \tag{6}$$

$$a_{1,1}(v) = -\frac{c_{\alpha,v}l_v^2 + c_{\alpha,h}l_h^2}{vJ} \tag{7}$$

$$a_{1,2} = -\frac{c_{\alpha,v}l_v - c_{\alpha,h}l_h}{J} \tag{8}$$

$$a_{2,1}(v) = -1 - \frac{c_{\alpha,v}l_v - c_{\alpha,h}l_h}{v^2m} \tag{9}$$

$$a_{2,2}(v) = -\frac{c_{\alpha,v} + c_{\alpha,h}}{vm}. \tag{10}$$

3.3 Steering Dynamics

The reference value δ_{ref} calculated by the MPC needs to be controlled by the subordinated steering angle controller inside the EPS. The purpose of the steering angle controller is to reproduce the steering inputs achieved today by a human driver. Work done by Beck (2017) using a conventional EPS system examines a wide range of measurement data to reproduce the full operational bandwidth of the steering system. Using the power spectral density to analyse the data in the frequency domain and plotting the integral of the power spectrum over frequency, it can be seen in figure 3, that the bandwidth of 3 Hz represents 99 % of the energy excitation within the steering system. This

is a realistic bandwidth that the steering angle controller should achieve.

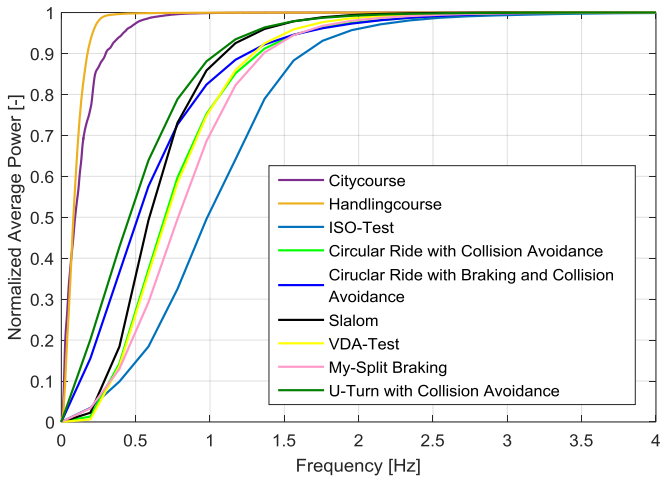

Fig. 3. Frequency analysis of representative driving manoeuvres

Work done by Govender et al. (2016) and Govender and Müller (2016) show a detailed approach to the problem of steering angle control for autonomous driving, however for the design of the MPC a linear model of the closed-loop steering angle controller dynamics is required. To this end a PT2 element with a cut-off frequency of 3 Hz is used (gain K, damping d and time constant T) that can be written in state-space representation

$$\frac{d}{dt}\begin{bmatrix}\delta\\ \dot{\delta}\end{bmatrix} = \begin{bmatrix}0 & 1\\ \frac{-1}{T^2} & \frac{-2d}{T}\end{bmatrix}\begin{bmatrix}\delta\\ \dot{\delta}\end{bmatrix} + \begin{bmatrix}0\\ \frac{K}{T^2}\end{bmatrix}\delta_{ref}. \tag{11}$$

3.4 Prediction Model in State-Space Representation

Summarizing equations (3), (6) and (11) the whole prediction model for the MPC corresponds to

$$\frac{d}{dt}\begin{bmatrix}\delta\\ \dot{\delta}\\ \dot{\psi}\\ \beta\\ \psi\\ dy\end{bmatrix} = \underbrace{\begin{bmatrix}0 & 1 & 0 & 0 & 0 & 0\\ \frac{-1}{T^2} & \frac{-2d}{T} & 0 & 0 & 0 & 0\\ \frac{c_{\alpha,v}l_v}{J} & 0 & a_{1,1}(v) & a_{1,2} & 0 & 0\\ \frac{c_{\alpha,v}}{vm} & 0 & a_{2,1}(v) & a_{2,2}(v) & 0 & 0\\ 0 & 0 & 1 & 0 & 0 & 0\\ 0 & 0 & l_v & v & v & 0\end{bmatrix}}_{\mathbf{A}_{dyn}(v)}\begin{bmatrix}\delta\\ \dot{\delta}\\ \dot{\psi}\\ \beta\\ \psi\\ dy\end{bmatrix} + \underbrace{\begin{bmatrix}0\\ \frac{K}{T^2}\\ 0\\ 0\\ 0\\ 0\end{bmatrix}}_{\mathbf{B}_{dyn}}\delta_{ref} + \underbrace{\begin{bmatrix}0\\ 0\\ 0\\ 0\\ 0\\ -v\end{bmatrix}}_{\mathbf{E}_{dyn}(v)}\Theta_{ref} \tag{12}$$

$$dy = \underbrace{\begin{bmatrix}0 & 0 & 0 & 0 & 0 & 1\end{bmatrix}}_{\mathbf{C}_{dyn}}\begin{bmatrix}\delta & \dot{\delta} & \dot{\psi} & \beta & \psi & dy\end{bmatrix}^T. \tag{13}$$

The velocity dependence of the matrices $\boldsymbol{A}_{dyn}(v)$ and $\boldsymbol{E}_{dyn}(v)$ results from the demand of a velocity adaptive lateral control. Through a range of $v = 1 - 30\,\mathrm{m/s}$, a set of matrices were calculated.

To analyze the transfer characteristics $G(s) = dy(s)/\delta(s)$, figure 4 shows the corresponding pole-zero plot for $v = 1 - 30\,\mathrm{m/s}$.

Due to the pole on the imaginary axis, the system is marginally stable. The impulse response corresponds to $\Theta_{ref} = 0$ to a linearly rising function. With increasing speed, the damping ratio decreases and the poles convert to a static position. The system still remains marginally stable.

The task of the MPC is, to stabilize the system on the reference path in compliance with manipulated variable constraints.

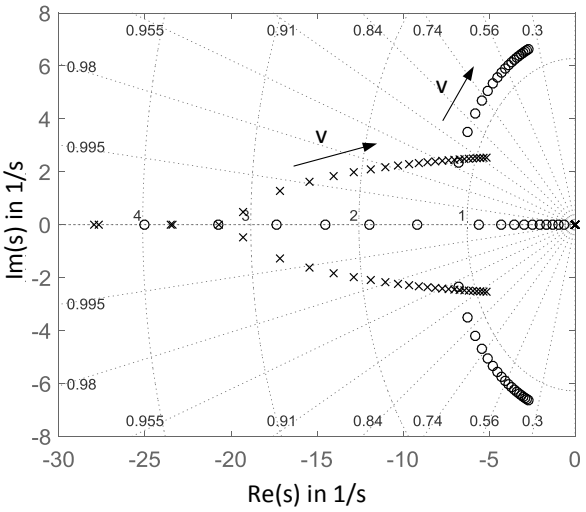

Fig. 4. Pole-zero plot of $G(s) = dy(s)/\delta(s)$

Substituting the dynamic single track model by the kinematic model, the reduced prediction model results to

$$\frac{d}{dt}\begin{bmatrix}\delta\\ \dot{\delta}\\ \psi\\ dy\end{bmatrix} = \underbrace{\begin{bmatrix}0 & 1 & 0 & 0\\ \frac{-1}{T^2} & \frac{-2d}{T} & 0 & 0\\ \frac{v}{l_v + l_h} & 0 & 0 & 0\\ v(\frac{1}{2} + \frac{l_v}{l_v + l_h}) & 0 & v & 0\end{bmatrix}}_{\mathbf{A}_{kin}(v)}\begin{bmatrix}\delta\\ \dot{\delta}\\ \psi\\ dy\end{bmatrix} + \underbrace{\begin{bmatrix}0\\ \frac{K}{T^2}\\ 0\\ 0\end{bmatrix}}_{\mathbf{B}_{kin}}\delta_{ref} + \underbrace{\begin{bmatrix}0\\ 0\\ 0\\ -v\end{bmatrix}}_{\mathbf{E}_{kin}(v)}\Theta_{ref} \tag{14}$$

$$dy = \underbrace{[0\ 0\ 0\ 1]}_{\mathbf{C}_{kin}} \left[\delta\ \dot{\delta}\ \psi\ dy\right]^T. \tag{15}$$

The characteristic polynomial of the state-space representations (14) and (15) becomes

$$p = \lambda^2(\lambda^2 + \lambda\frac{2d}{T} + \frac{1}{T^2}). \tag{16}$$

The zeros of the polynomial correspond to the eigenvalues of the system. One complex conjugate zero pair has a negative real-part, a double zero exists on the imaginary axis. Equivalent to figure 4, the system is also marginally stable but does not reflect the speed dependent system dynamics of the vehicle.

The following transformations apply equally to the dynamic and kinematic prediction model. Therefore the indices *kin* and *dyn* are no longer considered.

For the controller design, the matrices $\boldsymbol{B}$ and $\boldsymbol{E}(v)$ are combined to the input matrix $\boldsymbol{B}(v)$ and afterwards discretized with the sampling rate T_s according to Lunze (2014) with the equations

$$\boldsymbol{A}(v)_d = \mathrm{e}^{\boldsymbol{A}(v)T_s}, \quad \boldsymbol{B}(v)_d = \int_0^{T_s} \mathrm{e}^{\boldsymbol{A}(v)\alpha} d\alpha \boldsymbol{B}(v) \tag{17}$$

$$\boldsymbol{C}_d = \boldsymbol{C}, \quad \boldsymbol{D}_d = \boldsymbol{D}. \tag{18}$$

4. MODEL PREDICTIVE CONTROLLER

For comparative purposes, the presented prediction models are used to design two Model Predictive Controllers. Figure 5 shows the inner structure of the MPC. The blocks Kalman-Filter and prediction model include the discretized state-space representations represented by (12)-(13) and (14)-(15) respectively.

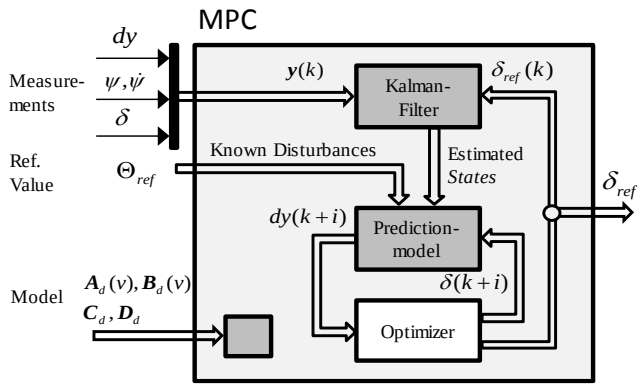

Fig. 5. Structure of the MPC

Before every prediction cycle the state vector of the predition model needs to be initialized with the measured plant outputs. Due to the sideslip angle being not available as a measured value and with all other measured outputs overlaid by interfering white noise, a Kalman-Filter is used to estimate all prediction model states. The Kalman-Filter and prediction model state space representations are adjusted, depending on the speed. The reference heading angle Θ_{ref} is perceived as an known disturbance input to the prediction model.

The optimizer minimizes the cost function J according to equation (19).

Constant parameters are chosed as follows:

- MPC sampletime: $T_{MPC} = 20\,\mathrm{ms}$
- Prediction horizon: $n_p = 50$
- Control horizon: $n_c = 20$
- Preview distance: $T_{prev} = T_{MPC} n_p = 1\,\mathrm{s}$
- Target value: $\delta_{target} = 0$

The variable k is the current control interval and i the index of summation.

$$\begin{aligned} J = & \underbrace{q \sum_{i=1}^{n_p} [(dy(k+i)]^2}_{J_{dy}} \\ & + \underbrace{r_1 \sum_{i=1}^{n_c} [\delta_{ref}(k+i-1) - \delta_{ref}(k+i-2)]^2}_{J_{\Delta\delta_{ref}}} \\ & + \underbrace{r_2 \sum_{i=1}^{n_c} [\delta_{ref}(k+i-1) - \delta_{target}(k+i-1)]^2}_{J_{\delta_{ref}}} \end{aligned} \tag{19}$$

The term J_{dy} weights the lateral displacement, $J_{\Delta\delta_{ref}}$ the steering angle rate and $J_{\delta_{ref}}$ the absolute steering angle.

The sample time T_{MPC} is equal to the sample time of the steering control input and therefore garantees a smooth setpoint change without destabilizing the steering angle control loop. The choice of T_{prev} is a compromise between the desired closed loop stability and the necessary processing performance required to compute a whole prediction cycle within T_{MPC} in real-time.

The input of the steering angle controller at the current control interval k is $\delta_{ref}(k) = \delta_{ref}(k-1) + \Delta\delta_{ref}(k)$ with the optimal control sequence

$$\Delta\boldsymbol{\delta}_{ref}(k) = \begin{bmatrix} \Delta\delta_{ref}(k) \\ \Delta\delta_{ref}(k+1) \\ \vdots \\ \Delta\delta_{ref}(k+n_c-1) \end{bmatrix} \tag{20}$$

is done by solving the differential equation

$$\min_{\Delta\boldsymbol{\delta}_{ref}(k)} J(\Delta\boldsymbol{\delta}_{ref}(k)) \Rightarrow \frac{\partial J(\Delta\boldsymbol{\delta}_{ref}(k))}{\partial \Delta\boldsymbol{\delta}_{ref}(k)} = 0 \tag{21}$$

subject to

$$\begin{aligned} \boldsymbol{\delta}_{ref,min} < \boldsymbol{\delta}_{ref}(k) < \boldsymbol{\delta}_{ref,max} \\ \Delta\boldsymbol{\delta}_{ref,min} < \Delta\boldsymbol{\delta}_{ref}(k) < \Delta\boldsymbol{\delta}_{ref,max}. \end{aligned} \tag{22}$$

Equation (21) represents a quadratic optimization problem. To assess the real-time capability, the computations

are performed on a dSpace MicroAutoBox II which consists of a PowerPC 750GL processor running at 900 Mhz. Because a sequence of quadratic programs need to be solved, the optimizer uses an active set method as QP-solver Schmid and Biegler (1994) and Camacho and Bordons (2007). With a turnaround time of approximately 5 ms, the MPC completed the prediction cycle within $T_{MPC} = 20$ ms and therefore in real-time.

5. SIMULATION RESULTS

To investigate the control behaviour, a nonlinear steering- and single track model were used. First analysis have shown, that stability and tracking performance are mainly influenced by the weights q and r_2. The weight r_1 changes the occurring lateral acceleration rate, which can be seen as a criteria for driving comfort Isermann (2006). This work however focuses on stability and tracking performance, therefore a constant weight of $r_1 = 1$ is chosen.

To examine the effects of the weights q and r_2 on the controller performance, a lane change maneuver according to Figure 6 is used. The maximum lateral displacement dy_{max} occurring during the maneuver is chosen as a criteria for the controller performance. The maneuver was performed for speeds from 2 to 20 m/s. For every speed the weights were varied to evaluate the influence on dy_{max}.

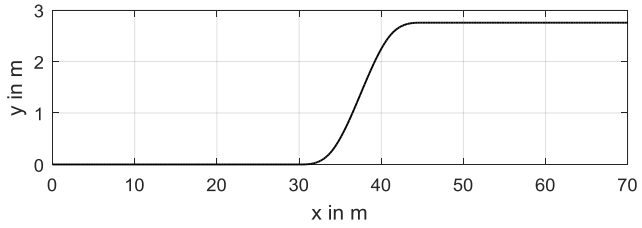

Fig. 6. Lane change maneuver

Figure 7 shows the simulation results for dy_{max} and the optimized speed dependent weights. Because the required steering angle increases notably at low speeds, it can be seen that a reduction of r_2 improves the tracking performance together with an increased weight q.

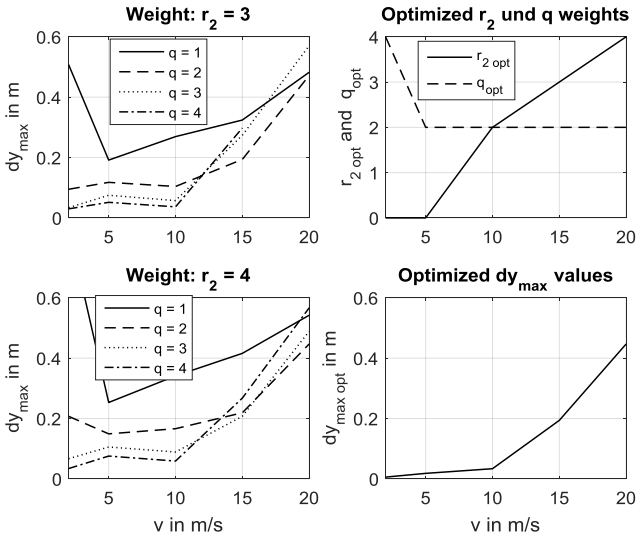

Fig. 7. Weight optimization

At higher speeds the weight r_2 stabilizes the vehicle by reducing the steering angle. Generally speaking, an increase of r_2 and a reduction of q increases the stability of the closed loop system, which on the other hand has a negative impact on the tracking performance at low speeds. Table 1 summerizes the relationship between vehicle speed, required steering angle and the resulting weights.

Table 1. Qualitative relationship between v and weights

v	Main challenge	δ_{ref}	r_2	q
low	path tracking	high	low	high
high	stability	low	high	low

To analyse the control behaviour at different curve radii, the handling track from figure 8 is used as reference path.

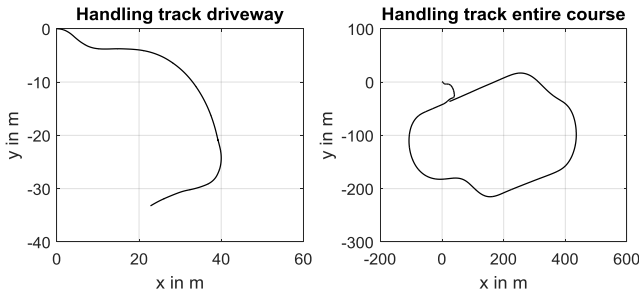

Fig. 8. Reference path

Minimum curve radii up to 8 m are built at the driveway of the handling track. This area is passed through with 2 m/s and the controller uses the optimized speed dependent weights r_2 and q. The curve radii during the following handling track vary between 48 m and 101 m.

Figure 9 shows the simulation results for the handling track driveway with different prediction models as a function of the arc length u. The solid line represents the dynamic single track model and the calculation of dy at the front axle according to figure 2.

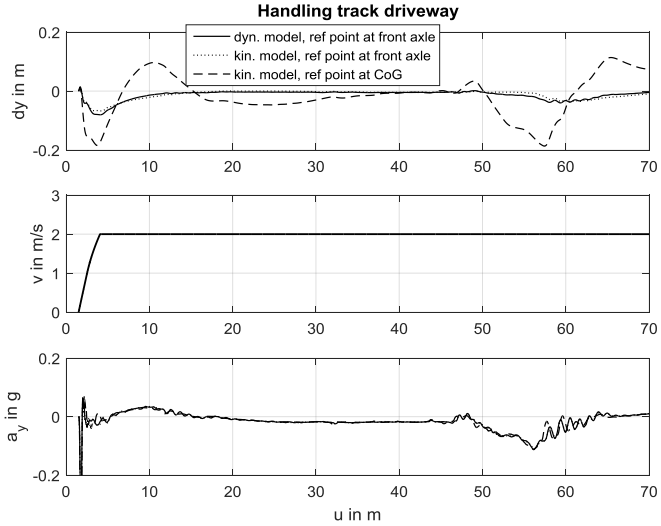

Fig. 9. Handling track driveway with optimized weights

The dotted line represents the kinematic single track model. Because of the low lateral acceleration, both prediction models show a similar tracking performance. The relationship $d\dot{y} = v(\psi + \beta - \Theta_{soll})$ can be used to predict the lateral displacement at the center of gravity instead of the front axle. It can be seen, that the chosen reference point has a significant impact on the tracking performance. The low curve radius in the driveway results in a significant change of dy along the length l_v. The predicted lateral displacement at the center of gravity differs from the measured one at the front axle which results in a deteriorated tracking performance.

Figure 10 shows the simulation results for curve radii up to 101 m. To evaluate the tracking performance at the limit of driving dynamics, a speed of 20 m/s for the handling track has been selected. Because of the high lateral accelerations, the kinematic single track model shows a poor performance.

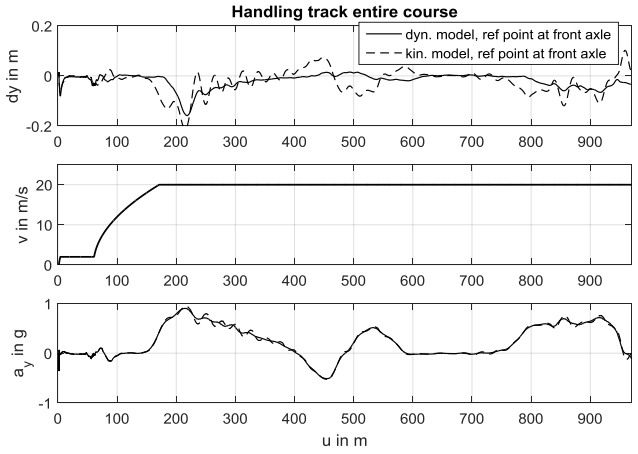

Fig. 10. Handling track with optimized weights

The resulting unprecise prediction of dy causes an increase of the lateral displacement. In comparison, the dynamic single track model shows also a good tracking performance for higher speeds.

6. CONCLUSIONS

In this paper, a model predictive controller for lateral vehicle guidance was presented, the influence of different prediction models was analyzed and a speed dependent weight optimization was implemented. The real-time capability was tested using a dSpace MicroAutoBox II. The controller showed a stable and smooth tracking with low lateral displacement for both low speeds with tight curves and highly dynamic maneuvers.

Further studies will focus on the analytical stability analysis of the closed loop system and the tradeoff between tracking performance and driving comfort.

REFERENCES

Beck, D. (2017). *Analysis and Specifications of a Fail-Operational EPS for Autonomous Driving.* Master's thesis, University of Applied Sciences Esslingen.

Camacho, E.F. and Bordons, C. (2007). *Model Predictive Control.* Springer Verlag, London.

Govender, V., Khazaridi, G., Weiskircher, T., and Müller, S. (2016). A PID and state space approach for the position control of an electric power steering. *16. Internationales Stuttgarter Symposium*, 755–769.

Govender, V. and Müller, S. (2016). Modelling and Position Control of an Electric Power Steering System. *8th IFAC Symposium on Advances in Automotive Control AAC 2016 Norrköping*, 49(11), 312–318.

Isermann, R. (2006). *Fahrdynamik-Regelung.* Vieweg & Sohn Verlag, Wiesbaden.

Katriniok, A. and Abel, D. (2011). LTV-MPC approach for lateral vehicle guidance by front steering at limits of vehicle dynamics. *IEEE Conference on Decision and Control*, 6828–6833.

Keviczky, T., Falcone, P., Borrelli, F., Asgari, J., and Hrovat, D. (2006). Predictive control approach to autonomous vehicle steering. *American Control Conference*, 4670–4675.

Lunze, J. (2014). *Regelungstechnik 2.* Springer Verlag, Berlin.

Mitschke, M. and Wallentowitz, H. (2014). *Dynamik der Kraftfahrzeuge.* Springer Verlag, Berlin.

Schmid, C. and Biegler, L. (1994). Quadratic programming methods for reduced hessian sqp. *Computers & Chemical Engineering*, 817–832.

Turri, V., Carvalho, A., Tseng, H.E., Johansson, K.H., and Borrelli, F. (2013). Linear model predictive control for lane keeping and obstacle avoidance on low curvature roads. *IEEE Annual Conference on Intelligent Transportation Systems (ITSC)*, 378–383.